Article

Modeling and Dynamic-Simulating the Water Distribution of a Fixed Spray-Plate Sprinkler on a Lateral-Move Sprinkler Irrigation System

Yisheng Zhang [1], Jinjun Guo [1], Bin Sun [1], Hongyuan Fang [1], Delan Zhu [2] and Huiliang Wang [1],*

[1] School of Water Conservancy and Science & Engineering, Zhengzhou University, Zhengzhou 450001, China; yishengzhang@zzu.edu.cn (Y.Z.); guojinjun@zzu.edu.cn (J.G.); sunbin@zzu.edu.cn (B.S.); fanghongyuan@zzu.edu.cn (H.F.)

[2] College of Water Resources and Architectural Engineering, Northwest A&F University, Yangling 712100, China; dlzhu@126.com

* Correspondence: wanghuiliang@zzu.edu.cn; Tel.: +86-0371-6778-1860

check for updates

Abstract: Uniformity of water distribution plays an important role in evaluating irrigation quality. As necessities in calculating irrigation uniformity during designing a lateral-move sprinkler irrigation system (LMSIS), the water distribution patterns of individual sprinkler in motion are crucial. Considering the limitation of the experiment platform, dynamic water distribution of an isolated sprinkler is difficult to measure, especially for a fixed spray plate sprinkler (FSPS) which LMSIS has been widely equipped with in China, therefore developing a model to simulate dynamic water distribution of a moving sprinkler is necessary. The objective of this study was to develop and validate the theoretical basis for calculating water distribution characteristics of a single FSPS in translational motion applying a superposition method, and provide an optimized operation management of LMSIS. The theoretical model's validity was verified in an indoor experiment using a Nelson D3000 FSPS in motion with 36 grooves and blue-plate spray heads. The software was programmed using the Eclipse Platform and the software was capable of simulating water distribution pattern and Christiansen uniformity coefficient (Cu). The results indicated that the water distribution simulated by the software presents three peaks of maximum application under varying conditions, and the value of water application peaks decreased as working pressure and/or mounting height increased. Conversely, the wetted diameter increased as working pressure and/or mounting height increased. Working pressure, mounting height, and sprinkler spacing each had a significant effect on the Cu. The Cu increased as working pressure and/or mounting height increased but decreased as sprinkler spacing increased. As a consequence, the model can be used to predict the relative water distribution pattern; and the Cu can be calculated with the simulated data, thus providing a tool for designing a new LMSIS.

Keywords: lateral-move sprinkler irrigation system; fixed spray plate sprinkler; dynamic simulation; water distribution characteristic; Christiansen uniformity

1. Introduction

Center-pivot and lateral-move sprinkler irrigation systems are widely used in agricultural applications, offering high levels of automation, reduced labor requirements, improved field microclimates, and water conservation [1–3]. In China, lateral-move sprinkler irrigation systems (LMSISs) play an important role in agricultural irrigation for the majority of rectangular fields. In order to decrease high energy consumption in a situation of energy scarcity, high working-pressure impact sprinklers have been replaced by low working-pressure sprinklers [4]. Commonly, two main low

working-pressure sprinklers are rotating spray-plate sprinklers (RSPSs) and fixed spray-plate sprinklers (FSPSs) [5,6]. Compared with RSPS, FSPS captured a host of consumers' attention for the advantages of lower working pressure, high wind resistance, and a low cost [7–9]. As a consequence, these systems are always equipped with a spray-plate sprinkler. Considering little information was provided by the producer, a slice of experiments for the exploration of water distribution has been conducted by researchers—the results imply that the static water distribution of FSPS resembles a wetted circular crown [7,10]. However, experimental exploration requires a series of experiments which is costly, labor-intensive, and time-consuming.

Recently, many simulation models were proposed for the optimal design of sprinkler irrigation systems. Carrón et al. [11] perfected the SIRIAS simulation model for a sprinkler system using ballistic theory, and the program can be used to calculate the uniformity of water distribution in windy conditions, therefore it is helpful for the design of a new sprinkler system. In order to simulate solid-set irrigation, Playán et al. [12] produced a simulation software based on a ballistic model to help irrigation professionals make a decision. Based on modified mathematical models and droplet evaporation theory, Li et al. [13] proposed a method for simulating droplet motion, furthermore, a software was developed to indicate water distribution pattern and water distribution uniformity. However, all these methods were used to simulate impact sprinklers other than FSPS. In order to obtain the unique water distribution of FSPS, Ouazaa et al. [14] simulated water distribution patterns for a fixed spray plate sprinkler using the ballistic theory, but the result demonstrates a large difference compared with the experimental method, and therefore it indicated that such a model might be more applicable to impact sprinklers which are attached to a solid-set sprinkler irrigation system.

As a consensus, the Christiansen uniformity coefficient (Cu) is commonly used to evaluate the water distribution uniformity of sprinkler irrigation systems [15–19]. In general, the Cu can be obtained by two ways: (1) Measure the water depth directly with an experimental method, and then calculate Cu with a designated formula; this method is always used to evaluate an existing system [20,21]. (2) Get the water distribution data of an isolated sprinkler, overlay water distribution of a single sprinkler for any number of sprinklers with different spacings, and then the Cu can be calculated. The second one is always applied to design a new system, and it has been previously investigated with some success [22]. Therefore, the second methodis applied more widely, which means that acquiring accurate water distribution pattern of a single sprinkler is paramount.

Commonly, during the calculation of Cu based on overlaying theory, the experimental methods of water distribution are completely different concerning variant irrigation systems. The calculation of water distribution uniformity of a solid-set sprinkler irrigation system is simple, for the only requirement is water distribution data of a single sprinkler under static state [23,24]. Different from permanent set sprinkler irrigation systems, the calculation of Cu of LMSIS is based on dynamic water distribution pattern [25–27]. Le Gat and Molle [28] presented a model for describing the application pattern of a single sprinkler based on calibrated statistical distributions, and the model can be used to calculate application patterns with a center pivot or lateral-move irrigation system equipped with impact sprinklers. In order to evaluate RSPS and FSPS in open field conditions, Faci et al. [7] measured static and dynamic water characteristics of individual sprinklers at different windy conditions, these data were mathematically overlapped to simulate the water distribution, the result indicated that RSPS attain a higher uniformity coefficient. Clark et al. [27] measured dynamic water distribution pattern of single FSPS, and then simulated water distribution and Cu by overlapping measured data, the result showed that simulated application patterns and Cu values compare well with field-measured patterns. These two studies demonstrated that the mathematical overlapping method can be used to simulate Cu as soon as the dynamic water distribution data of a single sprinkler were obtained. Considering the difficulty to determine mismatch of the farmland soil infiltration capacity, Liu [29] put forward to a calculation method of application depth and uniformity of LMSIS based on a dynamic irrigation procedure. However, the variable curve of water distribution used in this method should be measured with a LMSIS in advance, which is costly.

Considering the limitation of experiment platforms in measuring dynamic water distribution, developing a simulation model which can translate the static water distribution of one groove of FSPS to a dynamic water distribution of an individual sprinkler in motion is necessary. The objective of this study was to develop and validate the theoretical basis for determining dynamic water distribution of a sprinkler in motion using water distribution data from one groove of FSPS under static conditions. The theoretical model's validity was verified in an indoor experiment using a Nelson D3000 FSPS in motion with 36 grooves and blue-plate spray heads (Nelson Irrigation Co., Walla Walla, WA, USA). Based on the simulated water distribution patterns of an individual sprinkler under moving condition, different working pressures, mounting heights, and sprinkler spacings, Cus were calculated and recommendations were made to achieve optimum water distribution uniformity.

2. Calculation Theory

2.1. Theoretical Basis

To establish the theoretical basis proposed in this study, water depth data (collected using catch pans) for a single groove was initially used to determine the water distribution pattern of a sprinkler in motion. Assuming negligible differences among the grooves of FSPS and in the water distribution characteristics of dozens of single water jets [27,30], the water distribution pattern of other grooves was determined by changing the angles of the measured groove. When the sprinkler was in motion, the projected water depth of any one groove in the lateral direction was calculated separately. By superpositioning the projected water depth, the water distribution pattern of a sprinkler in motion was simulated.

Figure 1 illustrates the proposed sequential groove-by-groove process for determining the water distribution pattern from a sprinkler in motion for two grooves with angle, α. In this illustration, the water distribution cross sections of grooves 1 and 2 are shown separately and overlapped when the sprinkler is in motion. The projection and superposition method for determining the water distribution pattern for a sprinkler in motion is detailed below.
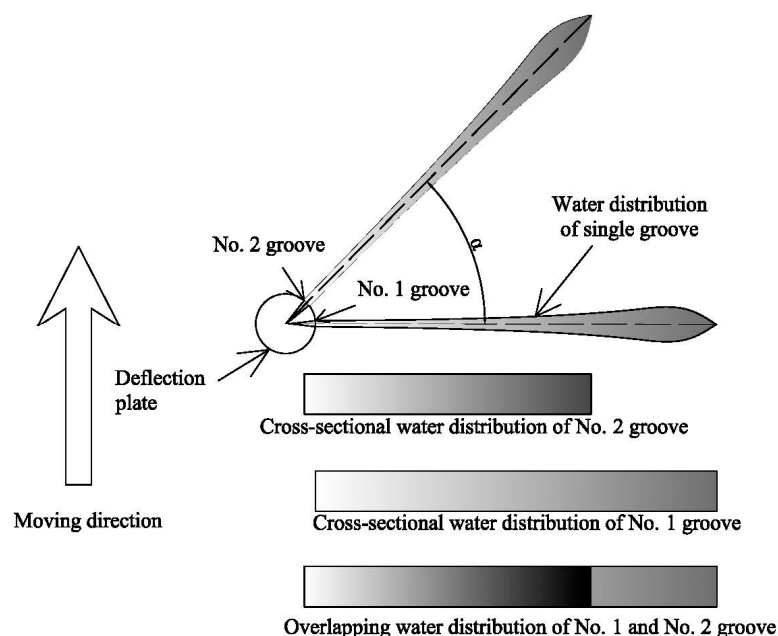

Figure 1. Sequential groove-by-groove process for determining the water distribution pattern from a sprinkler in motion.

(1)　Determine Water Distribution Pattern from a Single Groove

Figure 2 shows the coordinate system layout for determining the water distribution pattern from a single groove. The exact layout of the catch cans (with diameter, d) used to measure water depth is dependent upon the irrigation area. In this illustration, n is the number of rows, m is the number of columns, determined by the jet distance [7,8], and L is the distance between any two columns. Based on this coordinate system layout and the catch can characteristics, X- and Y-coordinate values were determined for the water depth measurements in each catch can in row n. Table 1 summarizes these coordinate values.
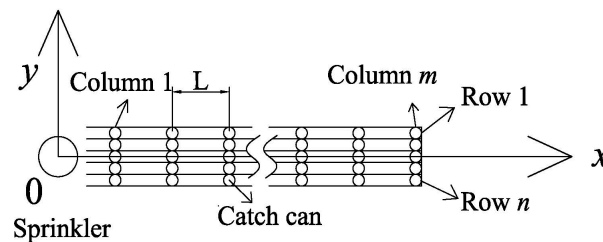

Figure 2. Coordinate system layout for determining the water distribution pattern from a single groove.

Table 1. X- and Y-coordinate values for the water depth measurements from a single groove.

Row	X-Coordinate Value	Y-Coordinate Value
1	$m \times L$	$(\frac{-n+1}{2} + 0) \times d$
2	$m \times L$	$(\frac{-n+1}{2} + 1) \times d$
3	$m \times L$	$(\frac{-n+1}{2} + 2) \times d$
n	$m \times L$	$(\frac{-n+1}{2} + n - 1) \times d$

(2) Apply Local Interpolation Method

Figure 3 shows this same coordinate system layout for a sprinkler in motion. In this illustration, the sprinkler is located at the point of origin and the water distribution section is initially parallel to the X-axis (Q_a position). Interpolation functions for the water depth, f, and spray distance, x, of each row were established as $f_{a1}(x)-f_{an}(x)$. When the groove was rotated counterclockwise by α (Q_b position), f and x of each row were changed to $f_{b1}(x)-f_{bn}(x)$.
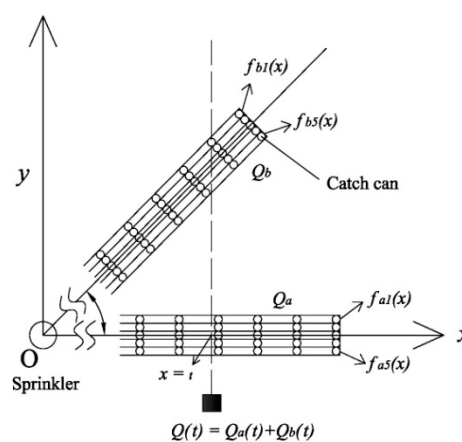

Figure 3. Coordinate system layout for determining the water distribution pattern from a sprinkler in motion.

Cubic spline interpolation has been widely applied when determining the water distribution patterns from sprinkler irrigation systems, offering smoothness and high accuracy [31,32]. However, noted issues including high radial variability in the water distribution of distinct jets, low water depths

near the sprinkler, and high concentrations of water in limited regions far away from the sprinkler [33] have resulted in negative water depths following cubic spline interpolation.

To address this issue, a local cubic spline interpolation method was used in which the water distribution curve was segmented and interpolation was performed on the individual segments to minimize variability and prevent negative water depth values. Figure 4 compares the results of this local interpolation method with the overall cubic spline interpolation method. As evident in the expanded view of Figure 4, the water depth increased sharply between points *a* and *b* and decreased sharply between points *b* and *c*. For the local cubic spline interpolation method, this water distribution curve was segmented into three segments: (1) section *a* preceded point *a*; (2) section *b* included points *a*, *b*, and *c*; and (3) section *c* followed point *c*. Cubic spline interpolation was performed separately for each of these three segments.
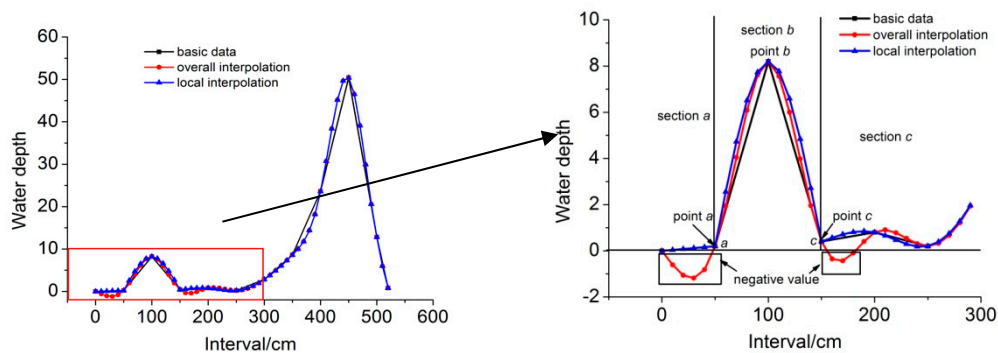

Figure 4. Comparison between overall and local cubic spline interpolation: direct view (**left**) and expanded view (**right**).

A local interpolation coefficient, *β*, was introduced for the purpose of determining the segments as follows:

$$\beta = \frac{f_{\max}(b)}{f_{\min}(a)} \tag{1}$$

where $f_{\max}(b)$ is the maximum value, $f_{\min}(a)$ is the minimum value, and *a* and *b* are the segment cutting points. When the value of *β* is fixed, the segment cutting point can be determined by comparing *β* to the maximum–minimum ratio. If the ratio value is larger than *β*, the segment cutting point is moved until the equality relationship is satisfied.

(3)　Overlap the Water Distribution Patterns of Different Grooves

As shown previously in Figure 3, the water distribution sections for grooves 1 and 2 of a sprinkler in motion were positioned at Q_a and Q_b. When the sprinkler is in motion, the overlapping water depth of grooves 1 and 2 at point *tm* can be calculated as follows:

$$Q(t) = Q_a(t) + Q_b(t) \tag{2}$$

$$Q_a(t) = \int_0^{(n-1)B} f_a(x)dx \tag{3}$$

$$Q_b(t) = \int_0^{(n-1)B} f_b(x)dx \tag{4}$$

where $Q_a(t)$ and $Q_b(t)$ are the accumulated water depths at point *tm* from grooves 1 and 2, respectively. Figure 5 shows the relative accumulated water depths by row at point *t*, $f_{b1}(t) - f_{bn}(t)$, from groove 2. The accumulated water depth for each row can be calculated as follows:

$$Q_b(t) = \int_0^{(n-1)B} f_b(x)dx = S_1 + S_2 + S_3 + S_4, \tag{5}$$

$$S_1 = \frac{f_{b1}(t) + f_{b2}(t)}{2} \times B, \tag{6}$$

$$S_2 = \frac{f_{b2}(t) + f_{b3}(t)}{2} \times B, \tag{7}$$

$$S_{n-1} = \frac{f_{b(n-1)}(t) + f_{bn}(t)}{2} \times B, \tag{8}$$

$$B = d/\cos(\alpha), \tag{9}$$

where B is the projection distance on Y-axis between any two adjacent rows at the same t location of groove b; α in Equation (9) is the angle between groove 1 and groove 2.

For the Nelson D3000 FSPS, this projection and superposition method was applied to consider each of its 36 grooves. Assuming negligible differences in water distribution among the grooves, this process based on the water distribution pattern of an individual sprinkler in motion should prove valid.
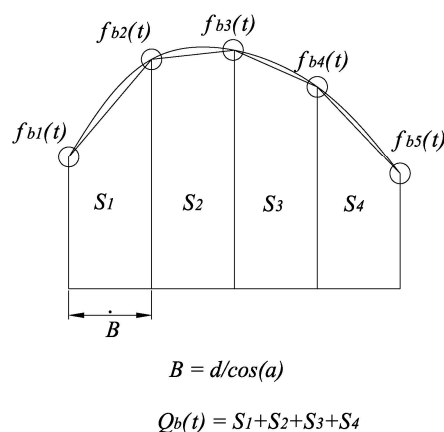

$$B = d/cos(a)$$

$$Q_b(t) = S_1 + S_2 + S_3 + S_4$$

Figure 5. Accumulated water depths by row from groove 2 at point tm.

2.2. Software Development

The software to simulate the dynamic water distribution pattern of FSPS was programmed with Java language. As shown in Figure 6, when the catch can parameters and application rate were obtained with the software, together with the interpolation parameters, the software meshed the water distribution data by row from the original groove using local cubic spline interpolation. As soon as the design parameters of FSPS were determined, the water distribution pattern could be calculated applying the projection and superposition method. The output data included relative water depth of FSPS in motion and/or in a static situation. Relative water distribution depth was calculated as follows:

$$Rd = \frac{h_i}{\sum\limits_{i=1}^{n} h_i} \tag{10}$$

where Rd is relative water distribution depth, h_i is simulated and/or experimental irrigation intensity.
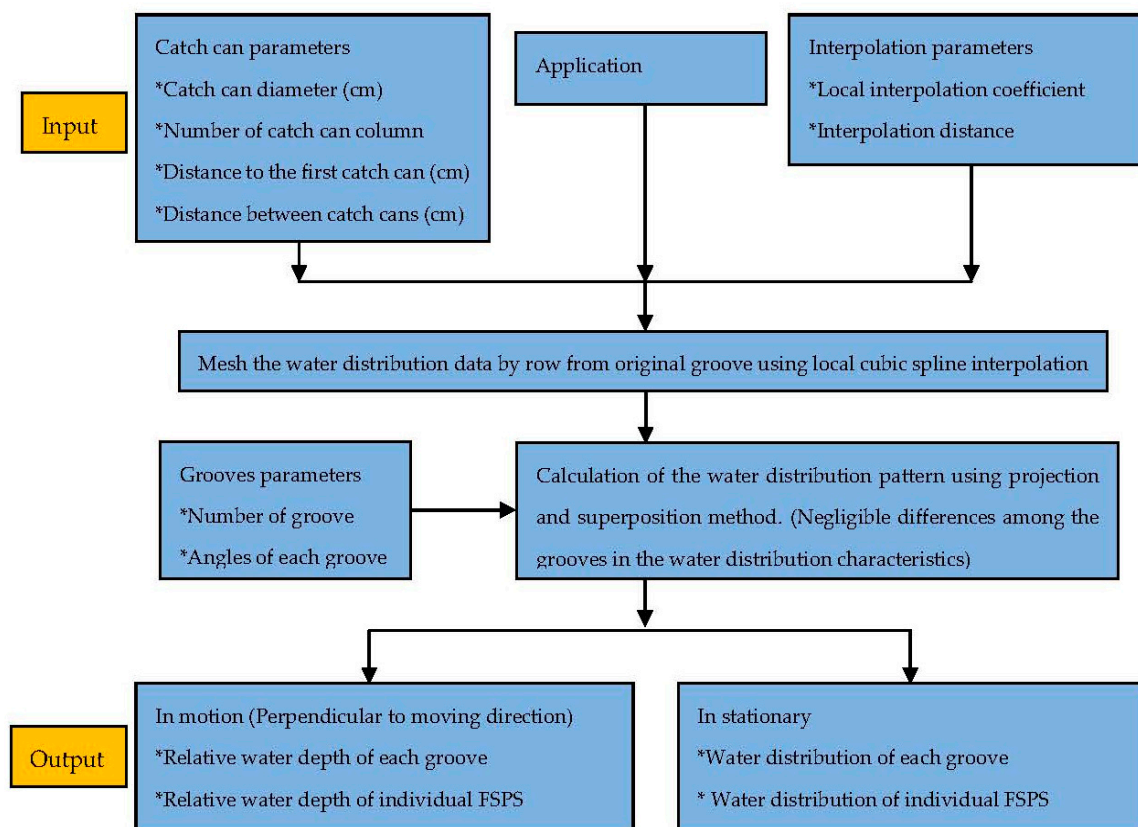
Figure 6. Calculation of water distribution pattern.

3. Validation and Application of the Theory

3.1. Verification Experiment

(1) Water Distribution Pattern from a Single Groove

To determine the water distribution pattern from a single groove, an experiment was performed using a sprinkler test platform located at the Irrigation Hydraulics Experiment Station, Northwest Agriculture and Forestry University, Yangling, China. A Nelson D3000 FSPS with spray head nozzle diameters of 4.76 mm was used in this experiment. Figure 7 shows the experimental setup. The water jet was captured in catch cans that had a height of 20 cm and an inside diameter of 17 cm. The catch cans were arranged along the jet direction. The distance between the catch can columns was 0.5 m except in areas of high water concentration where the distance between the catch can columns was 0.25 m.
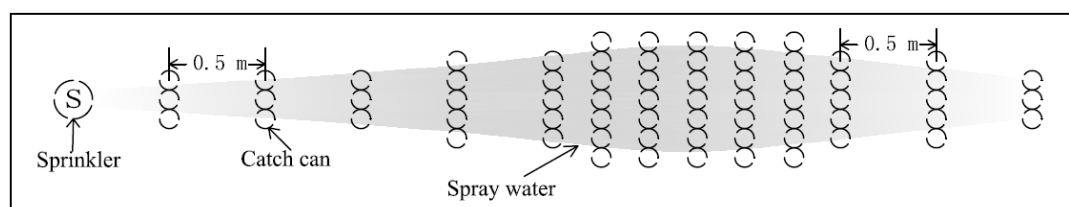

Figure 7. Experimental setup to determine the water distribution pattern from a single groove.

(2) Water Distribution Pattern from a Sprinkler in Motion

Using the proposed theoretical basis, the water distribution pattern from any groove of a sprinkler in motion with different jet angles could be determined once the water depth of a single groove was obtained. To verify the validity of this method, water conservation principles were applied to the

water jets with different rotating angles. Table 2 summarizes the measured water distribution pattern from a single groove with a 0° angle expressed as an application rate and based on the distance from the sprinkler at 1 m mounting height.

Table 2. Measured water distribution pattern from a single groove with 1 m mounting height.

Distance from Sprinkler (m)	Application Rate (mm·h^{-1})				
	Row 1	Row 2	Row 3	Row 4	Row 5
0	0	0	0	0	0
0.5	0	0.8	10.8	0.8	0
1	0	0.8	8.8	0.7	0
2	0	1.2	9.4	0.9	0
3	0	0.8	10.4	0.8	0
3.5	0	0.8	9.8	0.6	0
4	0	1.2	13.6	1.4	0
4.5	0	1.6	10.4	1.8	0
5	0	0.2	10.8	0.4	0
5.2	0	0.2	0.2	0.2	0

A second experiment was performed to determine the water distribution pattern from a sprinkler in motion. Figure 8 shows the experimental setup. The sprinkler was mounted on a traversing frame at 1.0 m above the catch cans. The catch cans were configured in a grid pattern comprising seven rows. The distance between the catch can columns was 0.5 m. A pressure gauge was installed upstream of the sprinkler spray heads and working pressures of 50, 100, 150, and 200 kPa were tested. A pump and a hose, which could be dragged by the traversing frame, supplied the water. The moving speed of the frame was 20 m/h.
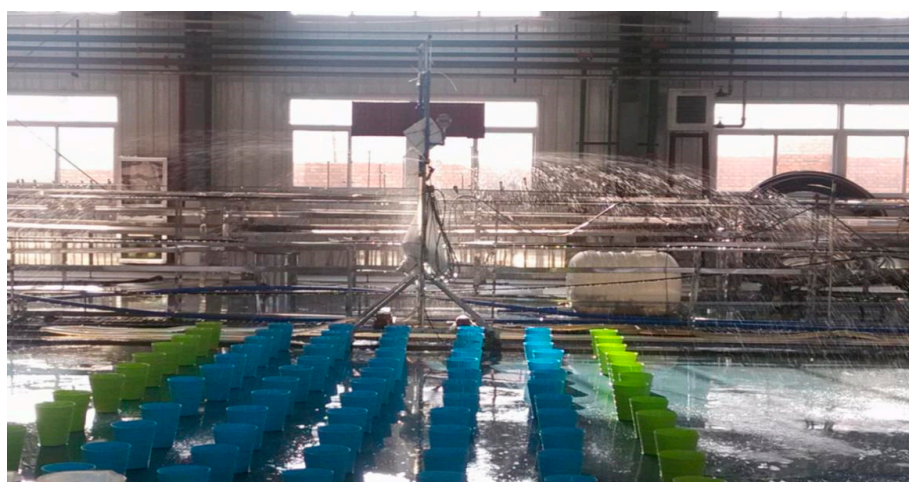

Figure 8. Experimental setup to determine the water distribution pattern from a sprinkler in lateral motion.

3.2. Application of Theory

The calculation theory was applied in order to get the single sprinkler water distribution data in lateral motion using a Nelson D3000 FSPS, and the data were used to calculate the uniformity with different working pressure, sprinkler spacing and mounting height. Table 3 presents the experimental factors and levels for simulation. The experiment to measure the water distribution data of single groove is presented in Figure 7. Combinations of 0.5, 1, 1.5, 2, and 2.5 m mounting heights and 50, 100, 150, and 200 kPa working pressures were tested. Each test lasted 1 h and was repeated five times.

Table 3. Experimental factors and levels for Christiansen uniformity coefficient (Cu) simulation.

Level	Factors		
	Working Pressure (kPa)	**Sprinkler Spacing (m)**	**Mounting Height (m)**
1	50	2	0.5
2	100	3	1
3	150	4	1.5
4	200	–	2
5	–	–	2.5

4. Results

4.1. Verification of the Theory

In a larger-scale experiment, the proposed theoretical basis was validated using a Nelson D3000 FSPS in a lateral motion. Figure 9 compares the measured and calculated relative water depths with working pressures of 50, 100, 150, and 200 kPa for a single sprinkler side. The calculated values were generally consistent with the measured values regarding spatial trends. Relative water depths decreased and converged to zero as the distance from the sprinkler increased for each of the working pressures considered. Fluctuations in the relative water depths indicated three peak application rates from the sprinkler. The measured relative water depths were 0–3.051, 0–2.157, 0–2.060, and 0–2.398 for working pressures of 50, 100, 150, and 200 kPa, respectively. Comparatively, the calculated water depth were 0–3.649, 0–4.456, 0–2.832, and 0–2.750 corresponding to 50–200 kPa. At different distances, a small difference could be observed with four working pressures. As shown in Figure 9a, with a distance of 0.5–1 m and 3–4 m from the sprinkler, the test data showed a downward trend, conversely, the simulated result of relative depth proposed a rising trend as the distance increased. Similar phenomenon could be observed with the other three working pressures, and part of the difference could be attributed to calculation error and experimental conditions, such as data conversion of different angles, slight changes in working pressure, and waggle of the moving frame. In addition, the simulated results at 0 m were always larger than the test value, this behavior would be explained by the waggle of the sprinkler during traversing frame moving, the peak application rate sprayed by the groove which was parallel to the moving direction transferred to adjacent area randomly. Simultaneously, it contribute to a larger measured value at 0–0.5 m as presented in Figure 9.

Table 4 summarizes the measured and calculated jet distances for working pressures of 50, 100, 150, and 200 kPa. In each case, the jet distance increased as the working pressure increased. The maximum deviation between the measured and calculated values was −12.50%, which was deemed acceptable. Calculation errors, pressure instability, and traversing frame quiver could each contribute to the magnitude of deviation.

Table 4. Comparison of measured and calculated jet distances for different working pressures.

Working Pressure (kPa)	Jet Distance (m)		
	Measured	**Calculated**	**Difference**
50	4.0	4.5	−12.50%
100	5.7	6.2	−8.77%
150	6.7	7.22	−7.76%
200	7.7	8	−3.90%

Despite small differences between measured and calculated relative water depths and jet distances, the proposed theoretical basis for estimating the water distribution pattern from a sprinkler in motion using data from a single groove appeared valid.
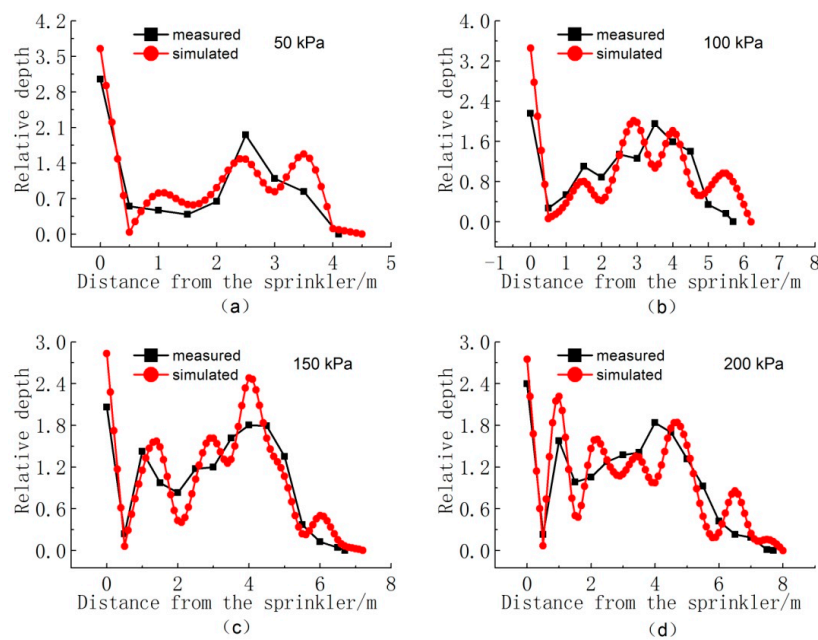
Figure 9. Measured and calculated relative water depths for the Nelson D3000 fixed spray-plate sprinkler (FSPS) in lateral motion with 1 m mounting height at different working pressures: (**a**) 50 kPa, (**b**) 100 kPa, (**c**) 150 kPa, and (**d**) 200 kPa.

4.2. Calculated Water Distribution Characteristics of Single Sprinkler in Motion

(1)   Water Distribution Pattern

Using the proposed theoretical basis, water distribution patterns from a sprinkler in motion were calculated using mounting heights of 0.5, 1, 1.5, 2, and 2.5 m and working pressures of 50, 100, 150, and 200 kPa. Figure 10 shows the effect of different working pressures (50–200 kPa) on the calculated relative water depths for the in-motion sprinkler mounted at 2 m. Figure 11 shows the effect of different mounting heights (0.5 to 2.5 m) on the calculated relative water depths for the in-motion sprinkler with a working pressure of 100 kPa.
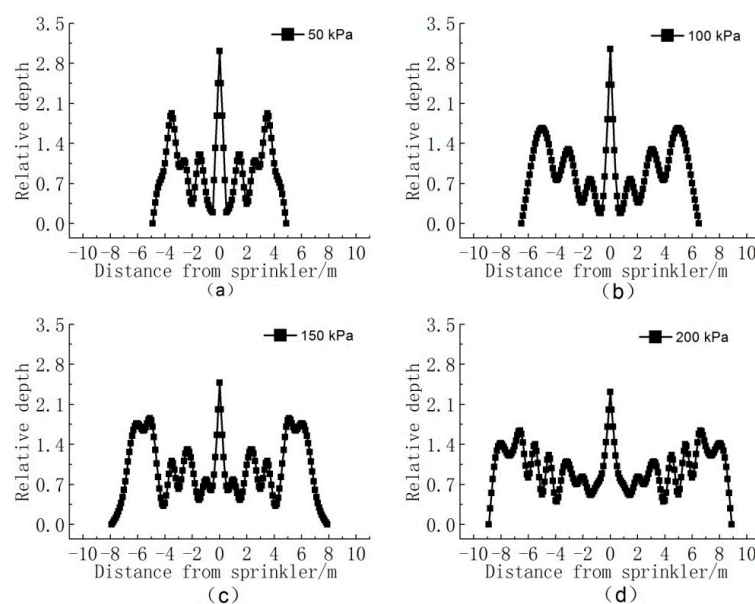

Figure 10. Calculated relative water depths for an in-motion sprinkler mounted at 2 m and at different working pressures: (**a**) 50 kPa, (**b**) 100 kPa, (**c**) 150 kPa, and (**d**) 200 kPa.
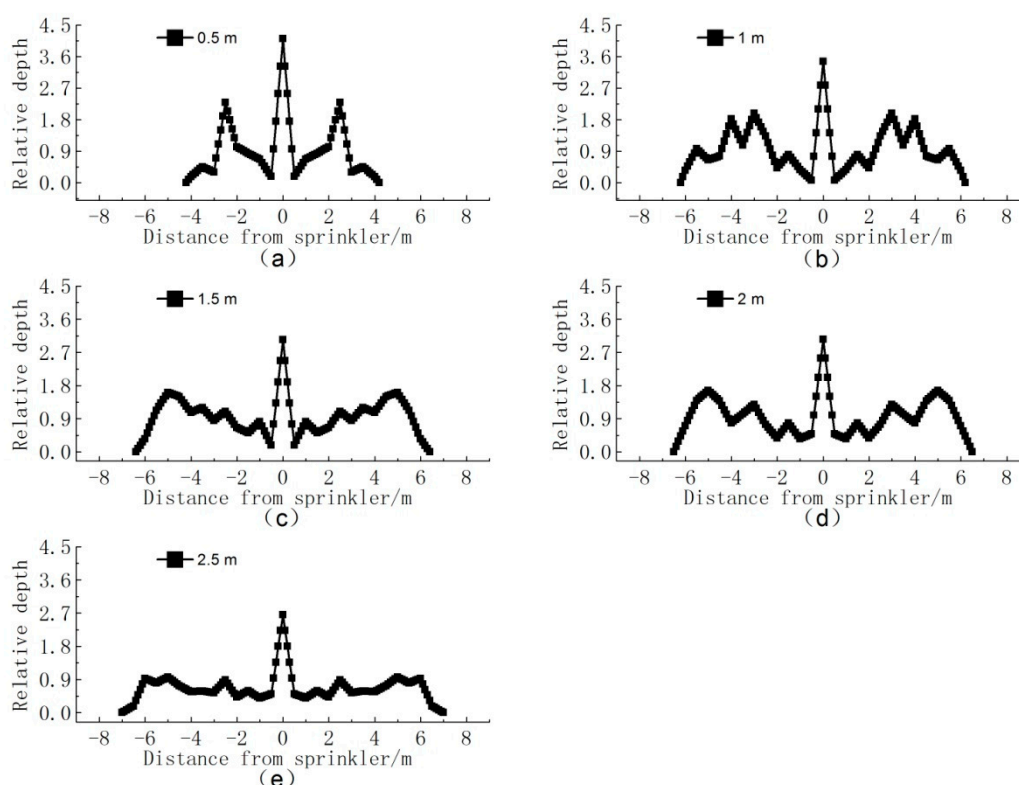
Figure 11. Calculated relative water depths for an in-motion sprinkler with a working pressure of 100 kPa and different mounting heights: (**a**) 0.5 m, (**b**) 1 m, (**c**) 1.5 m, (**d**) 2 m, and (**e**) 2.5 m.

(2)   Wetted Diameter

With respect to pressure effects, results indicated three peaks in water distribution that decreased as working pressures increased. The relative peak water depth on either side of the sprinkler was 1.922, 1.666, 1.82, and 1.581 for working pressures of 50, 100, 150, and 200 kPa, respectively. The relative peak water depth in the center of the sprinkler was 3.011, 3.050, 2.479, and 2.316 for the same working pressures.

With respect to mounting height effects, results indicated that the relative peak water depth decreased as the mounting height of the sprinkler increased. The relative peak water depth on either side of the sprinkler decreased from 2.292 with a mounting height of 0 m to 0.924 with a mounting height of 2 m. Similarly, the relative peak water depth in the center of the sprinkler decreased from 4.105 with a mounting height of 0.5 m to 2.658 with a mounting height of 2.5 m.

Wetted diameter is an important index that helps to determine appropriate sprinkler spacings. Using the same five mounting heights and four working pressures as above, Figure 12 shows the calculated wetted diameters for the sprinkler.

In general, as working pressure increased, the wetted diameter increased. For example, at a sprinkler mounting height of 2 m, the calculated wetted diameters were 4.9, 6.5, 7.9, and 8.9 m for working pressures of 50, 100, 150, and 200 kPa, respectively.

Similarly, the wetted diameter increased as the mounting height increased, although the rate of increase flattened for mounting heights >1 m. For example, at a constant working pressure of 50 kPa, the wetted diameter increased from 3 to 4.5 m as the mounting height increased from 0.5 to 1 m, representing a 50% increase in wetted diameter. At this same working pressure, the wetted diameter increased from 4.5 to 5.25 m as the mounting height increased from 1 to 2.5 m, representing a 16.7% increase in wetted diameter. When the mounting height was <0.5 m, increased working pressure could increase jet distance but the effectiveness for irrigation was unsatisfactory.
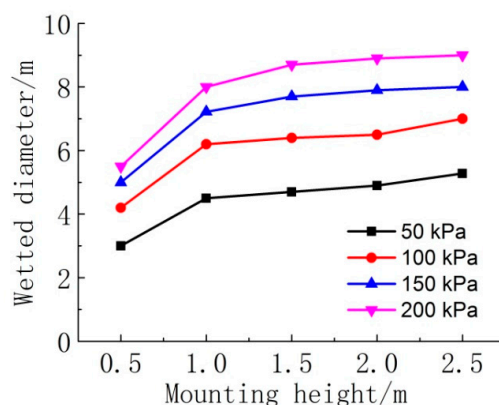
Figure 12. Calculated wetted diameters for an in-motion sprinkler with different working pressures and mounting heights.

4.3. Christiansen Uniformity

Cu is a key indicator for assessing irrigation quality, which is reflected in crop yield and water use efficiency. To calculate the Cu for a LMSIS, water distribution patterns were first determined by overlapping simulated single-sprinkler water distribution patterns using an interpolation interval of 0.1 m.

Figure 13 shows the calculated relative water depths for the Nelson D3000 FSPS for different working pressures and a fixed 2 m sprinkler mounting height and 3 m sprinkler spacing. The calculated relative water depths ranged from 0.61 to 1.60 for a working pressure of 50 kPa and from 0.89 to 1.12 for a working pressure of 200 kPa. As working pressure increased, the relative water depth ranges decreased, suggesting an increase in uniformity with an increase in pressure. In fact, the calculated Cu values were 76.72%, 78.85%, 77.87%, and 93.66% for working pressures of 50, 100, 150, and 200 kPa, respectively. These results are consistent with prior results reported by Clark et al. [27].
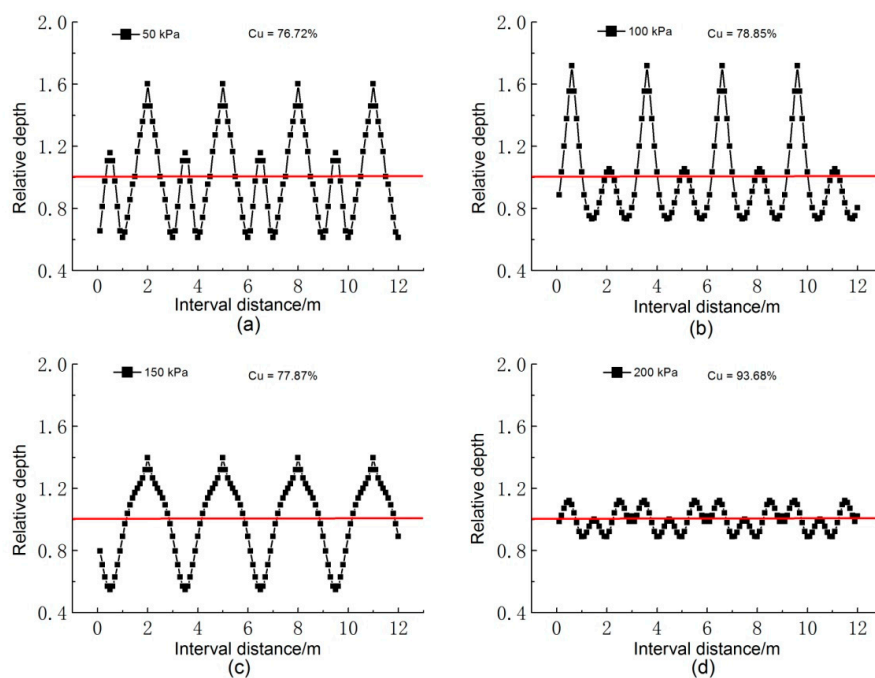

Figure 13. Calculated relative water depths for the Nelson D3000 FSPS with a 2 m sprinkler mounting height, 3 m sprinkler spacing, and different working pressures: (**a**) 50 kPa, (**b**) 100 kPa, (**c**) 150 kPa, and (**d**) 200 kPa.

Figure 14 presents a series of histograms depicting the calculated Cus as a function of sprinkler mounting heights (0.5, 1, 1.5, 2, and 2.5 m) and overlapping sprinkler spacings (2, 3, and 4 m) for different working pressure (50, 100, 150, and 200 kPa). These results indicated that the Cu values decreased as sprinkler spacing increased. Independent of mounting height, an increase in working pressure could increase Cu values. For example, with a fixed sprinkler spacing of 2 m, calculated Cu values were 19.59%, 71.24%, 71.59%, and 90.96% for working pressures of 50, 100, 150, and 200 kPa, respectively. A small increase in pressure resulted in a large change in the distribution pattern, which could subsequently affect the associated Cu value [27].
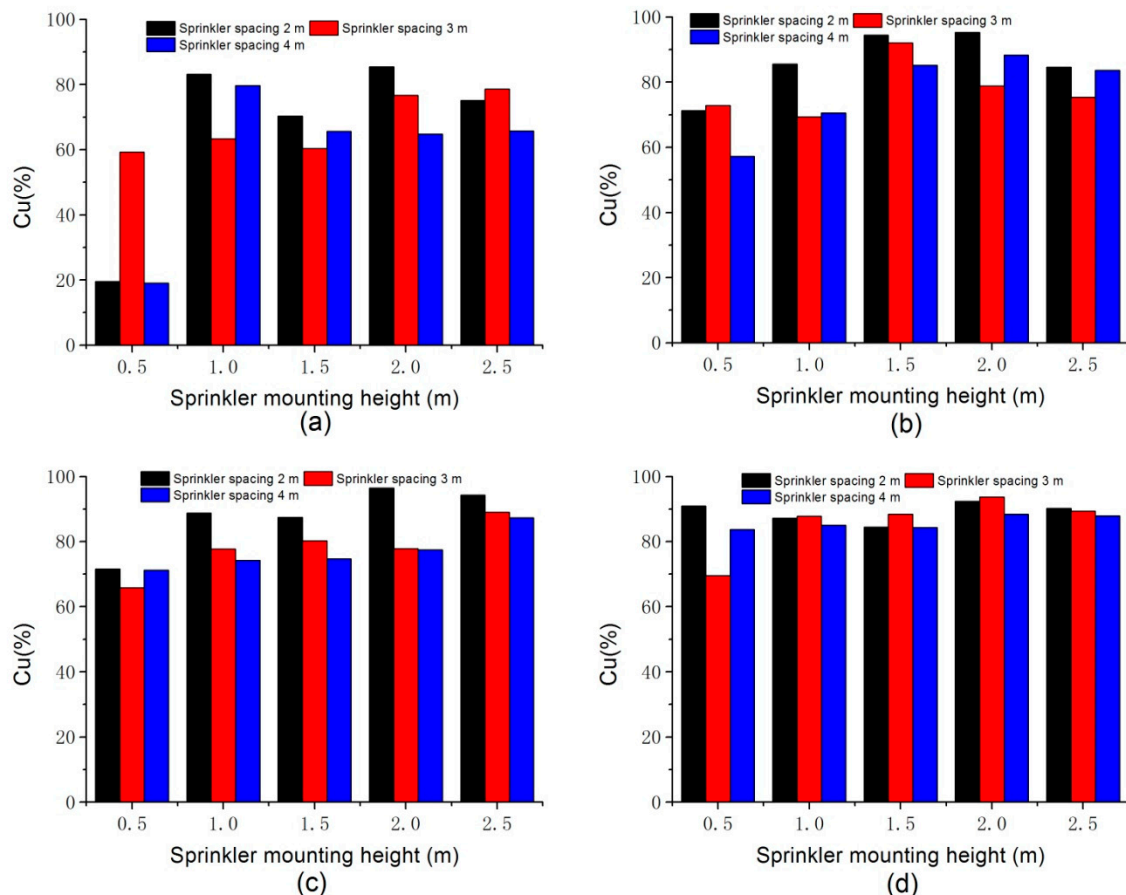

Figure 14. Calculated Cus as a function of mounting height and sprinkler spacing for different working pressure: (**a**) 50 kPa, (**b**) 100 kPa, (**c**) 150 kPa, (**d**) 200 kPa.

A more pronounced trend was observed between mounting height and Cu value. As mounting heights increased, Cu values increased. Poor uniformity was consistently observed at the 0.5 m mounting height with one exception: a Cu value of 90.2% was calculated for a working pressure of 200 kPa combined with a sprinkler spacing of 2 m. When the mounting height was >1.5 m, greater uniformity was consistently observed for each of the various sprinkler spacing–working pressure combinations.

5. Discussion

For the water distribution pattern simulated by the software was based on the water distribution data sprayed from one groove, it was vital to obtain the precise value of the target groove, even so, some differences between the simulated and experimental results could still be observed. These differences could be attributed to two aspects. The first one is calculation error; in general, small difference existed in each stream jetting from the grooves. But in this model, assuming negligible

differences among the different grooves, the water distribution pattern of other grooves was determined by changing the angles of the measured groove, and led to an idealized simulation result. The second one is experimental conditions, such as small pressure fluctuation, waggle of the frame. In addition, the moving speed might also have affected the differences; decreasing the frame moving speed resulted in an increasing of the water depth at a fixed measuring point, therefore it helped to reduce measuring error. Due to the limitation of insufficient experimental scenarios, the experiment of various frame moving speeds effecting on the measuring error was not conducted. Furthermore, the theoretical model's validity was verified in an indoor experiment using a Nelson D3000 FSPS in motion with 36 grooves and blue-plate spray heads, therefore the model validation for other types of fixed spray plate sprinkler should be investigated in the future. Nevertheless, the model could provide technical support for the calculation of water distribution of FSPSs.

Based on the simulated water distribution patterns of a sprinkler in motion with different working pressures, mounting heights, and sprinkler spacings, water distribution uniformities were calculated and recommendations were made to achieve optimum water distribution uniformity.

To fully analyze the direct and interactive effects of mounting height, sprinkler spacing, and working pressure on water distribution uniformity, an analysis of variance (ANOVA) was performed using the SPSS statistical software program. Table 5 summarizes the results of this analysis. This analysis confirmed (95% confidence interval) that each of these three factors affected the Cu. As indicated by the magnitude of associated F-values, working pressure, mounting height, and sprinkler spacing should be considered in priority order when higher levels of uniformity are required. However, higher working pressures are accompanied by higher energy and capital costs and thus, may not be the best first course of action. Comparatively, increased sprinkler mounting heights have no effect on costs, but are constrained in windy areas to avoid spray drift [16,34,35]. In windy areas, decreased mounting heights combined with decreased (more frequent) sprinkler spacing may provide the best results.

Table 5. Analysis of variance results.

Factors	Mean Square	F	Sig	Significance
Mounting height	945.522	10.685	0.000	***
Sprinkler spacings	308.043	3.466	0.039	**
Working pressure	1379.039	15.519	0.000	***

The levels for statistical significance adopted in this work were: $p < 0.10$ (*), $p < 0.05$ (**), $p < 0.001$ (***), or not significant (NS).

6. Conclusions

A theoretical basis for determining the water distribution pattern of FSPS in motion was developed in this study, and the validity was verified in an indoor experiment with Nelson D3000 FSPS. Using the proposed theoretical basis, various water distribution characteristics were next calculated. The results consistently indicated three water distribution peaks under varying conditions that decreased as working pressure and/or mounting height increased. Conversely, the wetted diameter increased as working pressure and/or mounting height increased.

Based on the simulated water distribution patterns of a sprinkler in motion with different working pressures, mounting heights, and sprinkler spacings, Cus were calculated and recommendations were made to achieve optimum water distribution uniformity. The results indicated that working pressure, mounting height, and sprinkler spacing each had a significant effect on the Cu. The Cu increased as working pressure and/or mounting height increased but decreased as sprinkler spacing increased.

Considering the limitation of insufficient experimental scenarios, the applicability of the model validation for other types of FSPS should be investigated in the future.

Author Contributions: Established the theoretical basis, Y.Z. Writing, original draft preparation, Y.Z. Writing, review and editing, J.G. and B.S. Funding acquisition, H.W. Performed the experiments, Y.Z. Software, D.Z. and Y.Z. Visualization, H.F. and H.W.

Conflicts of Interest: The authors declare no conflict of interest.

References

1. Clemmens, A.J.; Dedrick, A.R. *Irrigation Techniques and Evaluations Management of Water Use in Agriculture*; Springer: Berlin/Heidelberg, Germany, 1994; pp. 64–103.
2. Kincaid, D.C. Application rates from center pivot irrigation with current sprinkler types. *Appl. Eng. Agric.* **2005**, *21*, 605–610. [CrossRef]
3. Playán, E.; Mateos, L. Modernization and optimization of irrigation systems to increase water productivity. *Agric. Water Manag.* **2006**, *80*, 100–116. [CrossRef]
4. Musick, J.T.; Pringle, F.B.; Walker, J.D. Sprinkler and furrow irrigation trends—Texas High Plains. *Appl. Eng. Agric.* **1988**, *4*, 46–52. [CrossRef]
5. Hanson, B.; Orloff, S. Rotator nozzles more uniform than spray nozzles on center-pivot sprinklers. *Calif. Agric.* **1996**, *50*, 32–35. [CrossRef]
6. Hills, D.J.; Barragan, J. Application uniformity for fixed and rotating spray plate sprinklers. *Appl. Eng. Agric.* **1998**, *14*, 33–36. [CrossRef]
7. Faci, J.M.; Salvador, R.; Playán, E.; Sourell, H. Comparison of fixed and rotating spray plate sprinklers. *J. Irrig. Drain. Eng.* **2001**, *127*, 224–233. [CrossRef]
8. Playán, E.; Garrido, S.; Faci, J.M.; Galan, A. Characterizing pivot sprinklers using an experimental irrigation machine. *Agric. Water Manag.* **2004**, *70*, 177–193. [CrossRef]
9. Zhang, Y.; Sun, B.; Fang, H.; Zhu, D.; Yang, L.; Li, Z. Experimental and simulation investigation on the kinetic energy dissipation rate of a fixed spray-plate sprinkler. *Water* **2018**, *10*, 1365. [CrossRef]
10. Sayyadi, H.; Nazemi, A.H.; Sadraddini, A.A.; Delirhasannia, R. Characterising droplets and precipitation profiles of a fixed spray-plate sprinkler. *Biosyst. Eng.* **2014**, *119*, 13–24. [CrossRef]
11. Carrión, P.; Tarjuelo, J.; Montero, J. SIRIAS: A simulation model for sprinkler irrigation. *Irrig. Sci.* **2001**, *20*, 73–84. [CrossRef]
12. Playán, E.; Zapata, N.; Faci, J.M.; Tolosa, D. Assessing sprinkler irrigation uniformity using a ballistic simulation model. *Agric. Water Manag.* **2006**, *84*, 89–100. [CrossRef]
13. Li, Y.; Bai, G.; Yan, H. Development and validation of a modified model to simulate the sprinkler water distribution. *Comput. Electron. Agric.* **2015**, *111*, 38–47. [CrossRef]
14. Ouazaa, S.; Burguete, J.; Paniagua, M.P.; Salvador, R.; Zapata, N. Simulating water distribution patterns for fixed spray plate sprinkler using the ballistic theory. *Span. J. Agric Res.* **2014**, *12*, 850–863. [CrossRef]
15. Christiansen, J.E. Irrigation by sprinkling. University of California Agricultural Experiment Station. *Bulletin* **1942**, *670*, 124.
16. Tarjuelo, J.M.; Montero, J.; Honrubia, F.T.; Ortiz, J.J.; Ortega, J.F. Analysis of uniformity of sprinkle irrigation in a semi-arid area. *Agric. Water Manag.* **1999**, *40*, 315–331. [CrossRef]
17. Louie, M.J.; Selker, J.S. Sprinkler head maintenance effects on water application uniformity. *J. Irrig. Drain. Eng.* **2000**, *126*, 142–148. [CrossRef]
18. Silva, L.L. The effect of spray head sprinklers with different deflector plates on irrigation uniformity, runoff and sediment yield in a Mediterranean soil. *Agric. Water Manag.* **2006**, *85*, 243–252. [CrossRef]
19. Marjang, N.; Merkley, G.P.; Shaban, M. Center-pivot uniformity analysis with variable container spacing. *Irrig. Sci.* **2012**, *30*, 149–156. [CrossRef]
20. Dogan, E.; Kirnak, H.; Dogan, Z. Effect of varying the distance of collectors below a sprinkler head and travel speed on measurements of mean water depth and uniformity for a linear move irrigation sprinkler system. *Biosyst. Eng.* **2008**, *99*, 190–195. [CrossRef]
21. Faria, L.C.; Nörenberg, B.G.; Colombo, A.; Dukes, M.D.; Timm, L.C.; Beskow, S.; Caldeira, T.L. Irrigation distribution uniformity analysis on a lateral-move irrigation system. *Irrig. Sci.* **2019**, *37*, 195–206. [CrossRef]
22. Mateos, L. Assessing whole-field uniformity of stationary sprinkler irrigation systems. *Irrig. Sci.* **1998**, *18*, 73–81. [CrossRef]

23.   Zhang, L.; Merkley, G.P.; Pinthong, K. Assessing whole-field sprinkler irrigation application uniformity. *Irrig. Sci.* **2013**, *31*, 87–105. [CrossRef]

24.   Zhang, L.; Hui, X.; Chen, J. Effects of terrain slope on water distribution and application uniformity for sprinkler irrigation. *Int. J. Agric. Biol. Eng.* **2018**, *11*, 120–125. [CrossRef]

25.   Fukui, Y.; Nakanishi, K.; Okamura, S. Computer evaluation of sprinkler irrigation uniformity. *Irrig. Sci.* **1980**, *2*, 23–32. [CrossRef]

26.   Omary, M.; Sumner, H. Modeling water distribution for irrigation machine with small spray nozzles. *J. Irrig. Drain. Eng.* **2001**, *127*, 156–160. [CrossRef]

27.   Clark, G.A.; Srinivas, K.; Rogers, D.H.; Stratton, R. Measured and simulated uniformity of low drift nozzle sprinklers. *Trans. ASAE* **2003**, *46*, 321. [CrossRef]

28.   Gat, Y.L.; Molle, B. Model of water application under pivot sprinkler. I: Theoretical grounds. *J. Irrig. Drain. Eng.* **2000**, *126*, 343–347. [CrossRef]

29.   Liu, J.; Zhu, X.; Yuan, S.; Fordjour, A. Modeling the application depth and water distribution uniformity of a linearly moved irrigation system. *Water* **2019**, *11*, 827. [CrossRef]

30.   Ge, M.S.; Wu, P.; Zhu, D.; Ames, D.P. Comparison between sprinkler irrigation and natural rainfall based on droplet diameter. *Span. J. Agric. Res.* **2016**, *14*, 1201. [CrossRef]

31.   McKinley, S.; Levine, M. Cubic spline interpolation. *College Redwoods* **1998**, *45*, 1049–1060.

32.   Sarfraz, M.; Butt, S.; Hussain, M.Z. Visualization of shaped data by a rational cubic spline interpolation. *Comput. Graph.* **2001**, *25*, 833–845. [CrossRef]

33.   Yan, H.J.; Jin, H.Z.; Qian, Y.C. Characterizing center pivot irrigation with fixed spray plate sprinklers. *Sci. China Technol. Sci.* **2010**, *53*, 1398–1405. [CrossRef]

34.   Vories, E.D.; Von Bernuth, R.D. Single nozzle sprinkler performance in wind. *Trans. ASAE* **1986**, *29*, 1325–1330. [CrossRef]

35.   Seginer, I.; Kantz, D.; Nir, D. The distortion by wind of the distribution patterns of single sprinklers. *Agric. Water Manag.* **1991**, *19*, 341–359. [CrossRef]